European Heart Journal (2013) **34**, 201–210
doi:10.1093/eurheartj/ehs373

Mutations in the area composita protein αT-catenin are associated with arrhythmogenic right ventricular cardiomyopathy

Jolanda van Hengel[1,2†], Martina Calore[3†], Barbara Bauce[4], Emanuela Dazzo[3], Elisa Mazzotti[4], Marzia De Bortoli[3], Alessandra Lorenzon[3], Ilena E.A. Li Mura[3], Giorgia Beffagna[3], Ilaria Rigato[4], Mara Vleeschouwers[1,2], Koen Tyberghein[1,2], Paco Hulpiau[1], Evelien van Hamme[1], Tania Zaglia[5,6], Domenico Corrado[4], Cristina Basso[4], Gaetano Thiene[4], Luciano Daliento[4], Andrea Nava[4], Frans van Roy[1,2*], and Alessandra Rampazzo[3*]

[1]Department for Molecular Biomedical Research, VIB, Ghent University, Technologiepark 927, B-9052 Ghent, Belgium; [2]Department of Biomedical Molecular Biology, Ghent University, Ghent, Belgium; [3]Department of Biology, University of Padua, Via G. Colombo 3, 35131 Padua, Italy; [4]Department of Cardiac, Thoracic, and Vascular Sciences, University of Padua, Padua, Italy; [5]Department of Biomedical Sciences, University of Padua, Padua, Italy ; and [6]Venetian Institute of Molecular Medicine, Padua, Italy

Received 23 May 2012; revised 25 September 2012; accepted 10 October 2012; online publish-ahead-of-print 7 November 2012

Aims Arrhythmogenic right ventricular cardiomyopathy (ARVC) is a major cause of juvenile sudden death and is characterized by fibro-fatty replacement of the right ventricle. Mutations in several genes encoding desmosomal proteins have been identified in ARVC. We speculated that αT-catenin, encoded by *CTNNA3*, might also carry mutations in ARVC patients. Alpha-T-catenin binds plakophilins and this binding contributes to the formation of the area composita, which strengthens cell–cell adhesion in contractile cardiomyocytes.

Methods and results We used denaturing high-performance liquid chromatography and direct sequencing to screen *CTNNA3* in 76 ARVC patients who did not carry any mutations in the desmosomal genes commonly mutated in ARVC. Mutations c.281T > A (p.V94D) and c.2293_2295delTTG (p.del765L) were identified in two probands. They are located in important domains of αT-catenin. Yeast two-hybrid and cell transfection studies showed that the interaction between the p.V94D mutant protein and β-catenin was affected, whereas the p.del765L mutant protein showed a much stronger dimerization potential and formed aggresomes in HEK293T cells.

Conclusion These findings might point to a causal relationship between *CTNNA3* mutations and ARVC. This first report on the involvement of an area composita gene in ARVC shows that the pathogenesis of this disease extends beyond desmosomes. Since the frequency of CTNNA3 mutations in ARVC patients is not rare, systematic screening for this gene should be considered to improve the clinical management of ARVC families.

Keywords Sudden cardiac death • Arrhythmia • Cardiomyopathy • Cell adhesion molecules • Genetics

Introduction

Arrhythmogenic right ventricular cardiomyopathy (ARVC) (MIM # 107970) is an inherited cardiac disease characterized by progressive fibro-fatty myocardial replacement, primarily of the right ventricle. The main clinical features are structural and functional abnormalities of the ventricles, electrocardiographic depolarization/repolarization changes, re-entrant arrhythmias, and sudden death.[1–3]

† These authors contributed equally.

* Corresponding author. Tel: +39 049 8276208 (A.R.)/+32 9 3313640 (F.v.R.), Fax: +39 049 8276209 (A.R.)/+32 9 3313500 (F.v.R.), Email: alessandra.rampazzo@unipd.it (A.R.)/f.vanroy@dmbr.vib-ugent.be (F.v.R.)

Most of the pathogenic mutations in ARVC have been identified in genes encoding the desmosomal proteins plakoglobin (*JUP*), desmoplakin (*DSP*), plakophilin-2 (*PKP2*), desmoglein-2 (*DSG2*), and desmocollin-2 (*DSC2*).[4–11] Mutations in desmosomal genes have been identified in ~50% of the ARVC patients,[12] defining desmosomes as major factors in ARVC pathogenesis.

A recently described cardiac junction is the so-called area composita, which is a mixed-type junctional structure composed of both desmosomal and adherens junctional proteins.[13] In epithelial cells, adherens junctions provide specific cell–cell adhesion by linking E-cadherin to the actin cytoskeleton.[14] The cytoplasmic domain of E-cadherin binds the armadillo proteins β-catenin and plakoglobin, which in turn bind α-catenins. Alpha-catenins are cytoplasmic molecules thought to be indispensable for dynamic maintenance of tissue morphogenesis by integrating in the cadherin–catenin complex and by interacting with the F-actin cytoskeleton.[15–17] There are three α-catenin subtypes in mammals: the ubiquitously expressed αE-catenin, the neural αN-catenin, and αT-catenin, which is especially abundant in heart tissue and in the peritubular myoid cells of testis.[18] Both αT-catenin and αE-catenin are present in the area composita at the cardiac intercalated discs (ICD), as well as N-cadherin, one of the classic cadherins. Using yeast two-hybrid (Y2H) assays and co-immunoprecipitation, αT-catenin was shown to interact directly with PKP2, indicating a unique molecular amalgamation of adherens junctional and desmosomal proteins in the area composita.[19]

From this we speculated that mutations in *CTNNA3*, the gene encoding αT-catenin, may also cause ARVC.

Methods

Clinical evaluation

The study involved 76 index patients of Italian descent diagnosed with ARVC according to major and minor criteria established by the 2010 Task Force.[20] The control group consisted of 250 healthy and unrelated Italian volunteers (500 alleles). Clinical evaluation consisted of a detailed personal and family history, physical examination, 12-lead electrocardiogram (ECG), signal-averaged ECG (SAECG), 24-h Holter ECG, stress test, and two-dimensional echocardiography.

Mutation screening

Mutation screening of the *CTNNA3* gene was performed by denaturing high-performance liquid chromatography (DHPLC) and direct sequencing on 76 Italian index patients (52 males). Prior genetic studies excluded mutations in the ARVC genes *PKP2*, *DSP*, *DSG2*, *DSC2*, and *JUP* (data not shown).

Recruitment, examination, and procedures for collection of DNA samples were in accordance with the Declaration of Helsinki. All participating individuals gave informed written consent. Polymerase chain reaction primers flanking each exon of the human *CTNNA3* gene were designed by PRIMER3. Polymerase chain reaction primers and DHPLC conditions are described in Supplementary material online, *Table S1*. The amplicons were analysed by DHPLC using the WAVE Nucleic Acid Fragment Analysis System 3500HT (Transgenomic Ltd, NE, USA). Samples showing changes in a DHPLC pattern were directly sequenced. *CTNNA3* sequences were assembled, translated with SeqMan II (DNASTAR) and compared with a reference sequence NM_013266.

The control group was used to exclude the possibility that any detected variations are common DNA polymorphisms. All the controls were unrelated healthy volunteers from the general Italian population. Mutation screening was also performed on available family members of the probands in whom a *CTNNA3* mutation was detected.

A one-sided binomial test was performed to compare the percentage of patients carrying *CTNNA3* mutations relative to controls.

Construction of WT and mutant *CTNNA3* vectors

The Gateway entry clone pENTR207-hαTctn(179-2887) has been described.[19] Polymerase chain reaction-based site-directed mutagenesis was performed to obtain constructs with *CTNNA3* cDNA carrying the mutations p.V94D and p.del765L (for details, see Supplementary material online).

The Gateway entry clones pENTR207-hαTctn(179-2887_WT), pENTR207-hαTctn(179-2887_V94D), and pENTR207-hαTctn(179-2887_del765L) were transferred to pdGBKT7, pdGADT7, and pdEGFP by Gateway LR cloning (Invitrogen) to generate expression plasmids.

Yeast two-hybrid assay

The Matchmaker Gold Y2H system (Clontech) was used with the Y2HGold yeast strain for protein interaction tests. Cotransformants were obtained by standard methods,[21] and plated on minimal synthetic drop-out medium (SD) lacking leucine and tryptophan (SD –LW). After 3 days, colonies were picked and grown overnight in the SD –LW medium. Replica plates selecting for prey–bait interactions in transformed yeasts were made in SD medium lacking leucine, tryptophan, histidine, and alanine (SD –LWHA), but containing 70 mM potassium phosphate, and 50, 100, or 200 ng/mL Aureobasidin (AbA; Clontech). In some cases, 40 μg/mL 5-bromo-4-chloro-3-indolyl-β-D-galactopyranoside (X-GAL, Clontech) was added. For every assay, expression levels of both bait and prey proteins were analysed by immunoblotting (see below).

Cell cultures

For cell culture assays, mutagenised cDNA was transfected into HL-1 cardiac myocytes, neonatal rat cardiomyocytes, HEK293T, and MCF7/AZ cells.

Neonatal rat cardiomyocytes were isolated from Crl:(WI)BR-Wistar rats (Charles River Laboratories, Wilmington, MA, USA) at the age of 1–3 days as described.[22] All animal procedures were in accordance with the institutional guidelines for animal research. HL-1 cells, kindly provided by Dr W.C. Claycomb (New Orleans), were cultivated in Claycomb medium (Sigma) (for details, see Supplementary material online).

Transient transfection of cultured cells and immunofluorescent staining

Neonatal rat cardiomyocytes were transfected, by using TransFectin (Bio-Rad), with constructs expressing fusion proteins of enhanced green fluorescent protein (EGFP) with wild type (WT) αT-catenin, p.V94D mutant, or p.del765L mutant. HL-1 cells were transfected by using Lipofectamine 2000 (Invitrogen), MCF7/AZ cells were transfected with Fugene (Roche), and HEK293T cells were transfected by DNA calcium phosphate coprecipitation.

The cells were fixed and incubated with mouse monoclonal antibody anti-β-catenin (clone 6F9, Sigma, diluted 1:150) and anti-vimentin (clone V9, Dako, diluted 1:500). After thorough rinsing of the coverslips in PBS, rabbit anti-mouse-TRITC (Dako) or goat anti-mouse-Alexa 633 (Invitrogen) secondary antibody was applied. For aggresome

detection, HEK293T cells were stained with the ProteoStat Aggresome dye (Enzo Life Sciences, PA, USA).

Immunoblot analysis of yeast and HEK293T cell cultures

Proteins were extracted from 2 OD_{600} units of yeast cells.[23] Proteins were separated by SDS–PAGE and then immunoblotted with a polyclonal antibody raised against αT-catenin (rabbit pAb 952).[18] Blots were developed with enhanced chemiluminescence and autoradiography.

Proteins from transfected HEK293T cells were isolated by boiling for 5 min in Laemmli buffer, or by using RadioImmunoPrecipitation Assay buffer. Immunoblot bands were quantified using the Odyssey system from Li-Cor Biotechnology (Lincoln, NE, USA) (for details, see Supplementary material online).

Co-immunoprecipitation

Cell lysates were prepared in PBS containing 1% Nonidet P-40 and a protease inhibitor cocktail (Complete; Roche Diagnostics). The lysates were centrifuged and a sample containing 800 μg protein was incubated for 4 h with a GFP-specific polyclonal antibody (3E6, Invitrogen) or β-catenin-specific monoclonal antibody (cl14, BD, Transduction Laboratories), after which 50 μL of anti-mouse IgG Dynabeads (Invitrogen) was added. After incubation for 1 h, the beads were washed four times with lysis buffer diluted 1/10. Samples were analysed by SDS–PAGE and western blotting. Proteins were detected with primary monoclonal anti-GFP antibody (Roche) or polyclonal anti-β-catenin antibody (Sigma), followed by horseradish peroxidase-coupled anti-mouse Ig or anti-rabbit Ig secondary antibody (Amersham), and blots were developed with enhanced chemiluminescence.

Results

Detection of *CTNNA3* mutations

We performed an exon-by-exon analysis of the *CTNNA3* gene on 76 ARVC index patients (52 males, mean age 42 ± 12 years) who fulfilled the 2010 Task Force criteria for ARVC.[20] All patients were

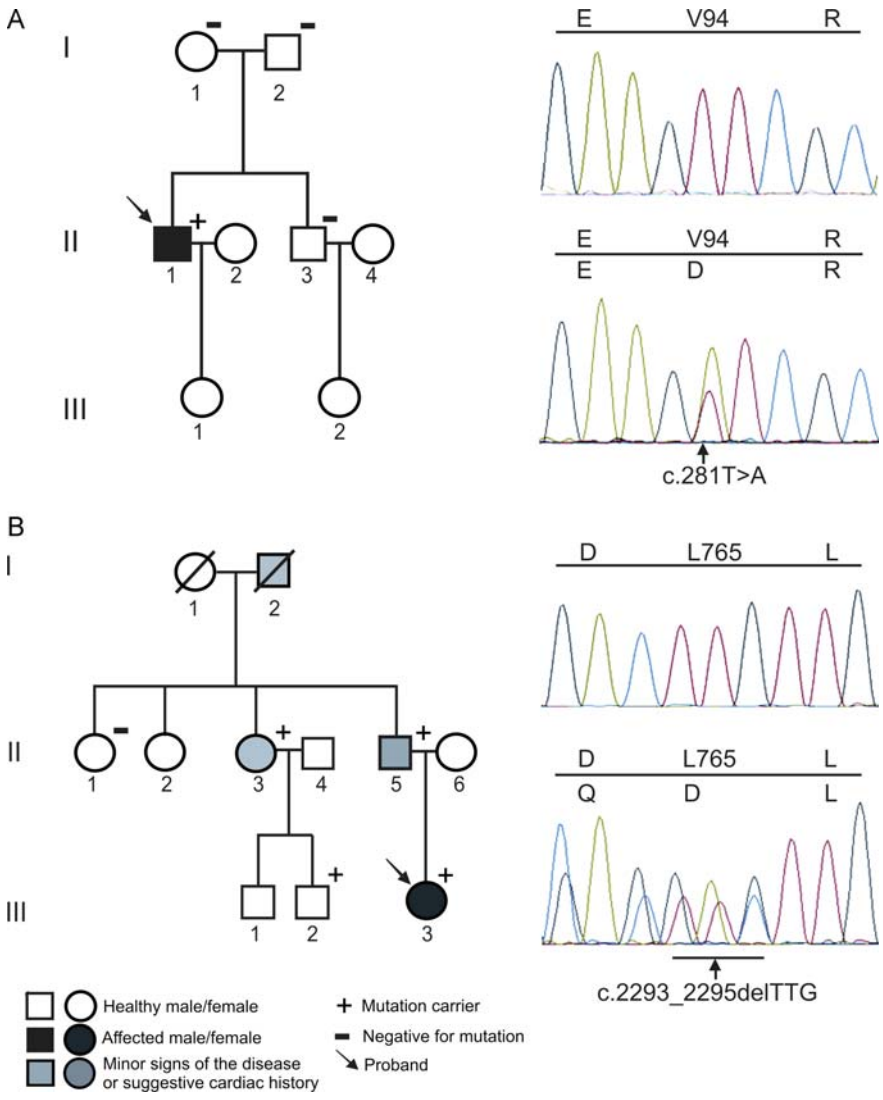

Figure 1 Family pedigrees of the patients with a *CTNNA3* gene mutation.

negative for mutations in the ARVC genes *PKP2*, *DSP*, *DSG2*, *DSC2*, and *JUP*. Two novel heterozygous mutations (c.281T > A and c.2293_2295delTTG) of *CTNNA3* were identified in two probands (*Figure 1*). These variants were not found in 250 ethnically matched healthy controls (500 chromosomes), in dbSNP (http://www.ncbi.nlm.nih.gov/projects/SNP/), in the 1000 Genomes Project database (http://www.1000genomes.org), or in the Exome Variant Server (http://evs.gs.washington.edu/EVS/). The frequency of *CTNNA3* mutation carriers in the 76 ARVC probands was 2.6% (95% CI: 0.0032–0.091; *P*-value for difference from the 250 Italian healthy controls = 0.04; *P*-value for difference from all the data available in the above-mentioned databases $<2.2 \times 10^{-16}$; binomial test, one-sided). The nucleotide substitution c.281T > A causes the amino acid change p.V94D, which was considered intolerant by SIFT (http://sift.jcvi.org/) and PolyPhen-2 (http://genetics.bwh.harvard.edu/pph2/) analysis. The variation c.2293_2295delTTG causes the deletion of leucine in position 765 (p.del765L). The missense mutation and the deletion are the first ARVC-associated *CTNNA3* mutations to be reported. They are both localized in important domains of αT-catenin, and the affected residues are strongly conserved among species (see Supplementary material online, *Figure S1*).

Clinical findings

In family A, male proband II,1 (*Figure 1*) was diagnosed at the age of 14 years during a screening for participation in sports activities. Basal ECG showed the presence of first degree atrioventricular block and negative T-waves in V1–V4 in the absence of complete right bundle-branch block (QRS ≥ 120 ms) (*Figure 2* and *Table 1*). He had several episodes of sustained ventricular tachycardia with left bundle-branch block (LBBB) morphology and superior axis deviation (*Figure 2* and *Table 1*). Late potentials were detected at 25, 40, and 80 filter setting, in the absence of a QRS duration ≥110 ms. Two-dimensional echocardiogram showed severe dilatation of the right ventricle with marked hypokinesia of the free wall, reduced right ventricular ejection fraction (RVEF), and anterior, apical and subtricuspid akinesia. Moreover, magnetic resonance imaging (MRI) showed a marked dilatation of the right ventricle, apical sacculation, and regional right ventricle akinesia with the RVEF of 30% (*Figure 2* and *Table 1*). After three transcatheter ablations, the patient received an implantable cardioverter defibrillator at the age of 36 years. The parents (I,1; I,2) and the brother (II,3) (*Figure 1*) were fully asymptomatic and do not carry the p.V94D mutation. Of note, the family history and genetic testing did not provide evidence that the cardiomyopathy of the proband was inherited.

Female proband III,3 in family B (*Figure 1*) was examined at the age of 15 years due to a syncopal episode. The ECG Holter showed non-sustained ventricular tachycardia with LBBB morphology and superior axis. Moreover, late potentials were present at 40 and 80 filter settings, in the absence of a QRS duration of ≥110 ms. Echocardiography showed mild right ventricular dilatation with kinetic abnormalities in the apical region (*Table 1*). Magnetic resonance imaging confirmed the presence of a mild

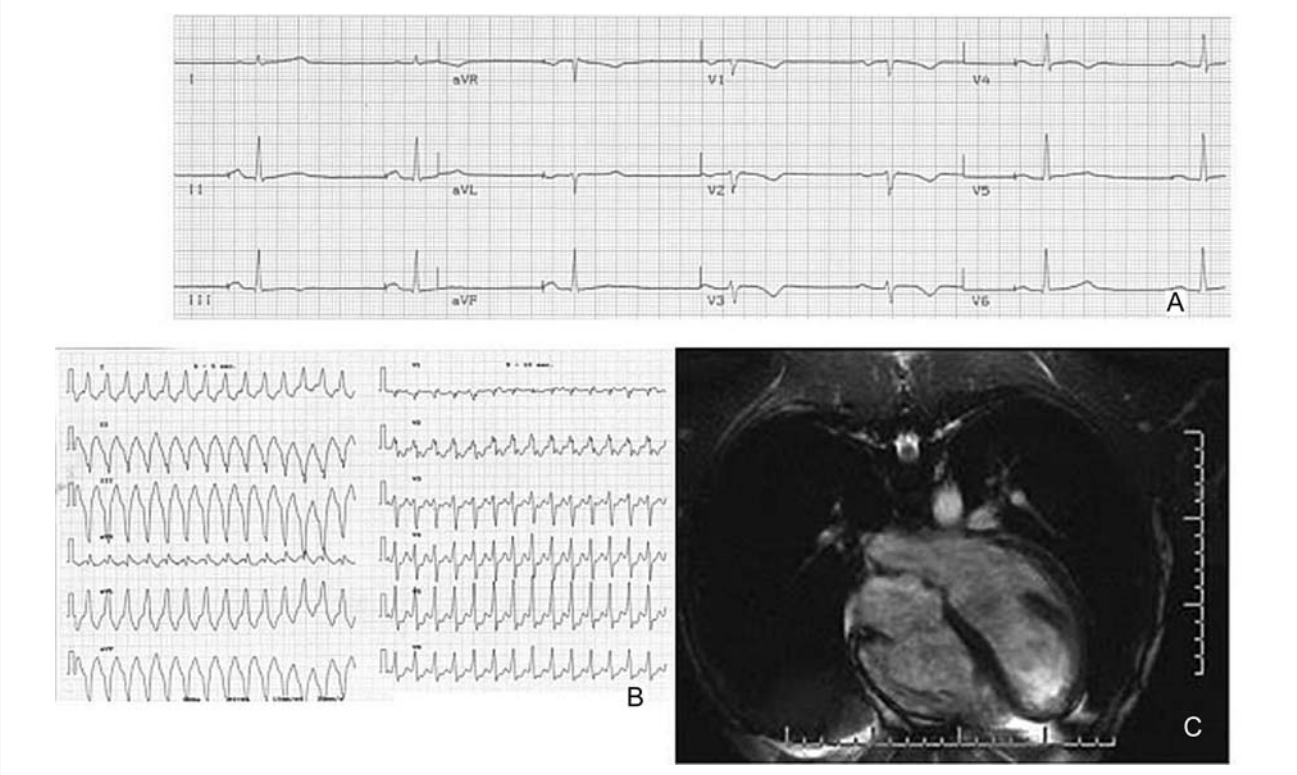

Figure 2 Clinical characteristics of the proband of family A. (*A*) 12-lead electrocardiogram showing first degree atrioventricular block and negative T-wave V1–V4. (*B*) Sustained ventricular tachycardia, with left bundle-branch block morphology and superior axis deviation. (*C*) Cardiac magnetic resonance demonstrating marked right ventricular dilation.

Table I Clinical data of probands and family members carrying *CTNNA3* mutations

Subject	Sex	Age at diagnosis/ investigation	Family history		12-lead ECG		SAECG	Arrhythmias		RV size/ function		LV involved	Diagnostic criteria	Mutation	
			M	m	Inverted T waves in right precordial leads	Epsilon wave		PVCs >500/24h NSVT	LBBB SVT	M	m			Nucleotide change	Amino acid change
Family A, II.1	Male	14 years	–	–	V1–V4	–	+	SVT	+	+	–	–	3 M/1 m	c.281T > A	p.V94D
Family B, III.3	Female	15 years	–	–	–	–	+	NSVT	+	–	+	–	1 M/2 m	c.2293_2295delTTG	p.del765L
Family B, II.5	Male	—	+	–	–	–	–	–	–	–	–	–	1 M	c.2293_2295delTTG	p.del765L
Family B, II.3	Female	—	–	+	–	–	–	–	–	–	–	–	1 m	c.2293_2295delTTG	p.del765L
Family B, III.2	Male	—	–	+	–	–	–	–	–	–	–	–	1 m	c.2293_2295delTTG	p.del765L

SAECG, signal-averaged electrocardiogram; PVCs, premature ventricular contractions; LBBB, left bundle-branch block; NSVT, non-sustained ventricular tachycardia; SVT, sustained ventricular tachycardia; RV, right ventricular; LV, left ventricle; M, major criteria; m, minor criteria.

dilatation of the right ventricle together with kinetic alterations of the right ventricular apex. She is currently undergoing antiarrhythmic therapy with Sotalol. Her father (II,5) (*Figure 1*), who carries the same mutation, does not fulfil the current diagnostic criteria for ARVC, but his echocardiogram demonstrates a mild right ventricular dilatation (PLAX RVOT = 30 mm). Subject II,3 (*Figure 1*) carries the p.del765L mutation and was asymptomatic, but contrast-enhanced MRI showed increased trabeculations in the right ventricular apex and intramural and epicardial fibrosis in the left ventricular posterolateral and basal inferior wall. Subject I,2 (*Figure 1*) died at the age of 83 years due to heart failure, without a history of valvular or ischaemic cardiac disease. Subject III,2 (*Figure 1*), who carries the same mutation, was asymptomatic, in line with the incomplete penetrance of the disease.[24]

Differential binding of WT and mutated αT-catenin

Alpha-T-catenin can interact with plakophilins PKP1, PKP2, and PKP3.[19] These interactions were confirmed in an improved Y2H assay (Matchmaker Gold, Clontech) (*Figure 3A*, rows 1 and 4). Interactions between αT-catenin and β-catenin or plakoglobin were also confirmed (*Figure 3A,* rows 7 and 10). In the same assay, the p.V94D and p.del765L mutants interacted normally with PKP3 and PKP2 (*Figure 3A*, rows 2, 3, 5, and 6). In contrast, the interaction of the p.V94D mutant with β-catenin or plakoglobin was quite weak compared with WT (*Figure 3A*, rows 8 and 11), whereas the p.del765L mutant still interacted normally with these armadillo proteins (*Figure 3A*, rows 9 and 12). The β-catenin binding site of the related human αE-catenin comprises residues 54–148 (see Supplementary material online, *Figure S1A*).[25]

Next, to test in mammalian cells whether the interaction of the p.V94D mutant with β-catenin was weaker than the WT interaction, endogenous β-catenin in HEK293T cells was co-immunoprecipitated with exogenous GFP–αT-catenin fusion protein (*Figure 4A*, left part). Co-immunoprecipitation was also done in the other direction (*Figure 4A*, right part). In both experimental setups, the interaction between p.V94D proteins and full-length β-catenin was much diminished.

Also homodimerization of αT-catenin was assessed in the Gold Y2H assay. The relative ability of Gold Y2H strains to grow in the presence of increasing concentrations of AbA reflects the strength of the interaction between bait and prey proteins. The homodimerization potentials of WT αT-catenin and p.V94D seemed rather weak because higher levels of AbA in the growth medium prevented yeast growth (*Figure 3B*, rows 1 and 2, columns C–E). In contrast, p.del765L showed a much stronger homodimerization potential than WT (*Figure 3B*, row 3). As the ARVC probands are heterozygous for their *CTNNA3* mutation, we also checked the interaction between the mutants and WT αT-catenin (*Figure 3B*, rows 4–7). We found that this interaction as well was stronger for the p.del765L mutant. This feature could lead to a dominant negative or dominant positive effect of p.del765L. We also tested whether αT-catenin interacts with αE-catenin, but neither WT nor mutant αT-catenin showed detectable interaction with αE-catenin in the Y2H assay (data not shown).

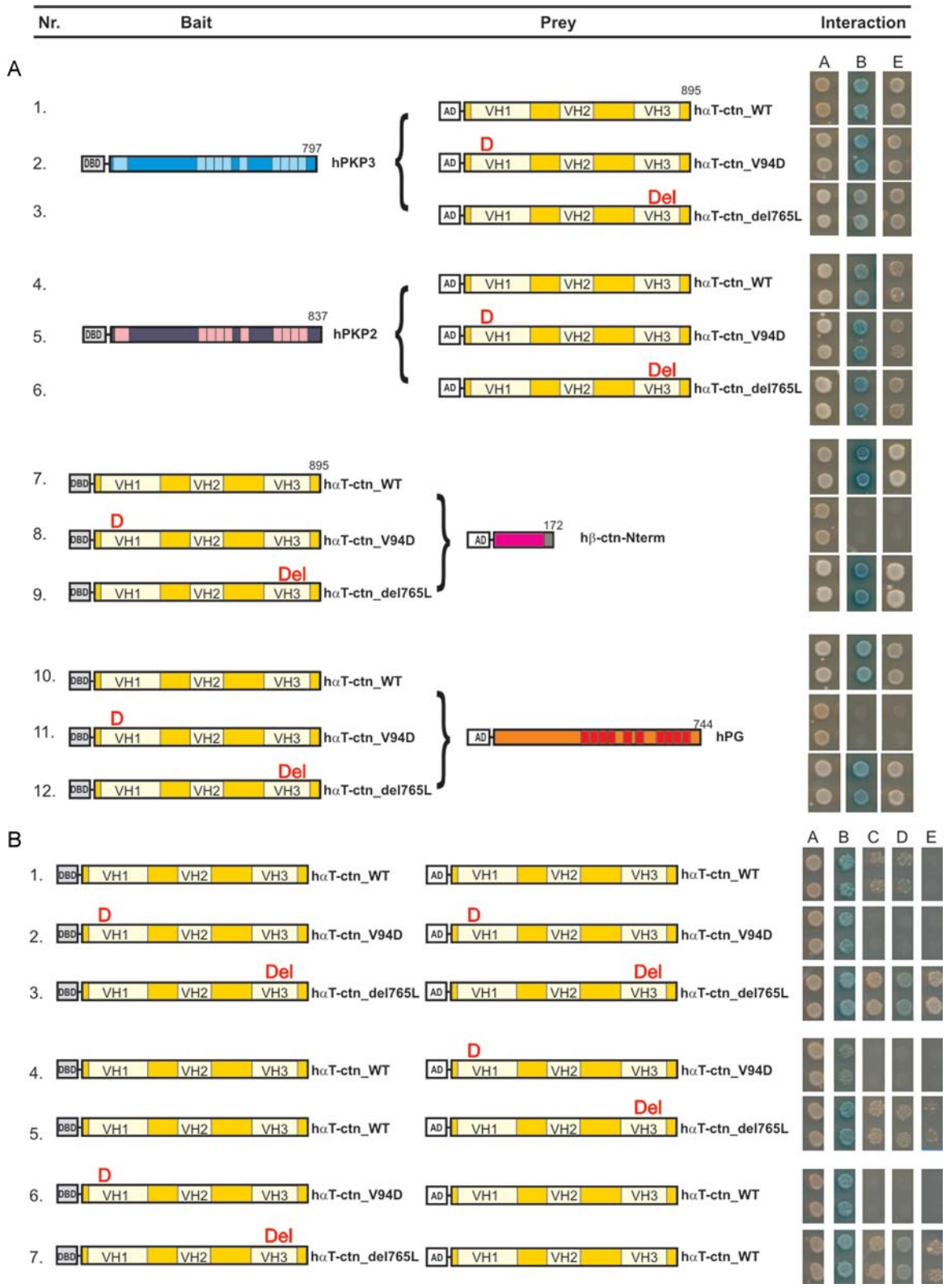

Cellular localization of αT-catenin

To assess whether the p.V94D and p.del765L mutations affect subcellular localization of αT-catenin, we expressed WT αT-catenin and the mutants as EGFP-fusion proteins. Constructs were transiently transfected into neonatal rat cardiomyocytes (*Figure 4B*) and into the mouse cardiac muscle cell line HL-1 (see Supplementary material online, *Figure S2*). In both cell types, WT and mutant p.del765L fusion proteins were detected at cell–cell contacts, where they colocalized with endogenous β-catenin. In contrast, the fusion protein carrying the p.V94D mutation was predominantly and consistently localized in the cytoplasm. No difference in the distribution of plakoglobin, plakophilin-2, or F-actin was observed (data not shown).

In addition, we took advantage of the capacity of overexpressed exogenous αT-catenin to form thread-shaped structures in MCF7/AZ cells (see Supplementary material online, *Figure S3*). This capacity was preserved in the p.V94D mutant. The amino-terminal part of β-catenin colocalized with the threads formed by WT αT-catenin but not with the threads containing the p.V94D mutation, confirming in mammalian cells that the interaction of the p.V94D mutant protein with β-catenin is crippled.

The stronger dimerization potential of p.del765L in yeast could mean that it is more stable than WT αT-catenin. In transformed yeast cells, chimaeric GAL4-αT-catenin protein levels were, however, similar for WT, p.V94D, and p.del765L (data not shown). We then addressed protein stability by cycloheximide treatment of transfected HEK293T cells. We noticed no differences in stability (data not shown), but the amount of solubilized p.del765L turned out to be strikingly less in RIPA lysates than in Laemmli buffer lysates (*Figure 5A*). Interestingly, microscopic evaluation of HEK293T transfectants revealed that the p.del765L mutant protein had an aggregate-like appearance unlike WT or p.V94D proteins (*Figure 5B and 5C*). Apparently, these p.del765L aggregates were less soluble in RIPA buffer. They fulfilled all criteria of aggresomes[26] by being pericentriolar structures different from ER, Golgi, and lysosomes, and recruiting a so-called vimentin cage (*Figure 5D*). The p.del765L aggregates also stained positive for Proteostat, an amyloid-specific red fluorescent dye (*Figure 5E*).[27] Recent evidence indicates that the mechanisms involved in the assembly of cytoplasmic protein aggresomes might differ in different cell lines.[28] Indeed, we did not observe prominent aggregates of this type in several other cell lines transfected with p.del765L. We also noticed that the WT protein was present in the aggresomes if the HEK293T cells expressed both WT and p.del765L protein (*Figure 5F*).

Discussion

We provide here the first description of αT-catenin mutations associated with a human disease. The two probands we identified fulfil the current ARVC diagnostic criteria and their clinical phenotype is identical to that reported in ARVC patients carrying typical desmosomal gene mutations. However, in the heart, αT-catenin is present only in the areae compositae.[19] In a previous study, the *CTNNA3* gene was evaluated in a family with dilated cardiomyopathy showing linkage to chromosomal region 10q21, but no *CTNNA3* mutations were detected.[29] More recently, Christensen *et al.*[30] performed mutation screening on 55 Danish patients fulfilling ARVC diagnostic criteria and found the rare p.A689V variant of *CTNNA3* in one patient, but they considered that the significance of this variant is unknown because they also found it in 2 out of 1400 controls.

It is not clear exactly how the *CTNNA3* mutations we report here perturb the assembly and function of the areae compositae in ARVC hearts. Germline knockout of αT-catenin in the mouse alters PKP2 distribution without affecting other junctional components of the areae compositae.[31] These mutant mice exhibit progressive dilated cardiomyopathy, gap junction remodelling, and increased sensitivity to ventricular arrhythmia following acute ischaemia, but not spontaneous ARVC. We speculate that the expression in cardiomyocytes of the mutant αT-catenins reported here might have a more drastic effect than full abrogation of αT-catenin. Mutant αT-catenins might lead to much weakened junctions between adjacent cardiomyocytes and to disruption of tissue integrity, particularly in response to excessive mechanical stress (e.g. competitive sports). This pathogenetic hypothesis would also explain why ARVC mostly involves the thin-walled areas of the right ventricle, which are structurally more vulnerable to mechanical stress.

Figure 3 Arrhythmogenic right ventricular cardiomyopathy-associated mutations in αT-catenin protein interfere with its binding properties. Matchmaker Gold yeast two-hybrid analysis was performed on WT and mutants of αT-catenin (yellow), and on the armadillo proteins PKP3 (blue), PKP2 (purple), N-terminal part of β-catenin (magenta), and plakoglobin (PG, orange). Armadillo repeats are depicted in contrasting colours. Data are shown each time as two representative yeast colonies. The yeast colonies shown in column A on the right were grown on SD −LW selection medium. In the Y2HGold yeast strain used, rescued GAL4 regulates the selection and reporter genes *ADE2*, *HIS3*, *MEL1*(α-galactosidase), and *AUR1-C*. This allows reliable detection of bimolecular interactions by formation of blue colonies on SD −LWHA (H, histidine; *A*, adenine) containing X-Gal (column *B*). *AUR1-C* expression confers strong resistance to Aureobasidin. Yeast colonies shown in columns C-E were grown on SD −LWHA containing 50 ng/mL Aureobasidin (*C*), SD −LWHA containing X-Gal and 100 ng/mL Aureobasidin (*D*), or SD −LWHA containing 200 ng/mL Aureobasidin (*E*). (*A*) Both the p.V94D and p.del765L mutants interact with PKP3 and PKP2. The p.del765L mutant still interacts with β-catenin and plakoglobin, but the p.V94D mutant interacts neither with β-catenin nor with plakoglobin (rows A8 and A11). Combinations involving bait constructs of β-catenin or plakoglobin could not be assessed due to the autoactivation observed when they were tested against prey vectors containing no insert. Numbers indicate the protein sizes (in amino acids) of the cloned catenin or plakophilin fragments. AD, GAL4 transcription activation domain; DBD, GAL4 DNA-binding domain; h, human; VH, vinculin homology domain. (*B*) p.del765L has a much stronger dimerization potential, both as homodimer (row B3) and as heterodimer with WT αT-catenin (rows B5 and B7). See (*A*) for annotations. All figures represent data from three or more independent experiments.

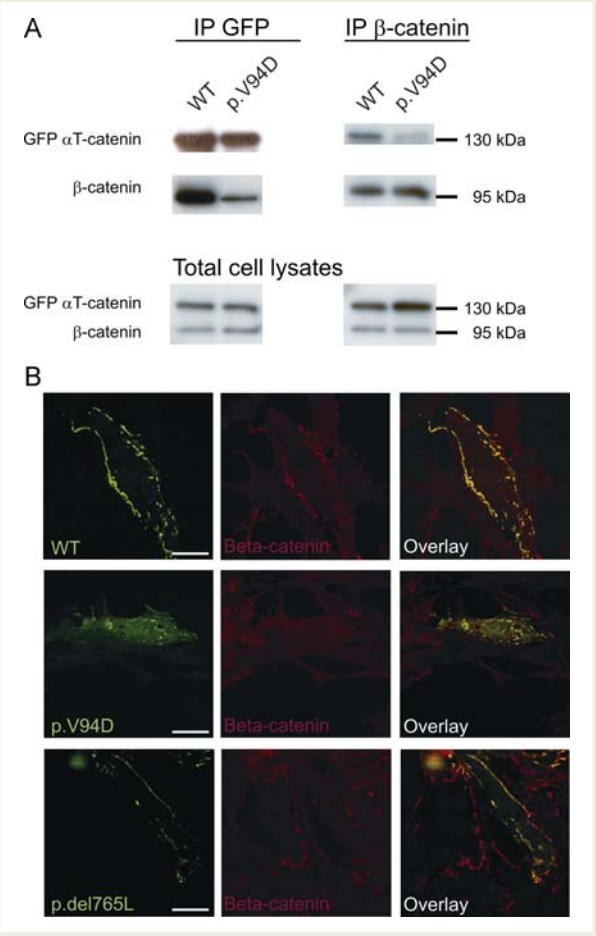

Figure 4 The interaction between αT-catenin and β-catenin is affected by the p.V94D mutation. (*A*) Left: GFP-fused WT or p.V94D αT-catenin proteins were immunoprecipitated from equal amounts of HEK293T cells transfected with appropriate constructs. Immunoprecipitates were blotted with either anti-GFP antibody or with anti-β-catenin antibody. Right: in an independent reverse experiment, endogenous β-catenin was immunoprecipitated from equal amounts of HEK293T cells transfected with constructs encoding GFP-fused αT-catenin. Reduced levels of coprecipitated GFP-fused p.V94D were detected when compared with GFP-fused WT αT-catenin. (*B*) Confocal microscopy of neonatal rat cardiomyocytes transfected with constructs expressing protein fusion of EGFP with WT αT-catenin, p.V94D mutant, or p.del765L mutant, as indicated. In each case, immunostaining for endogenous β-catenin was also performed. Note that the WT and p.del765L proteins are concentrated at the cell membrane, where they colocalize with β-catenin. In contrast, p.V94D is mainly distributed through the cytoplasm and not colocalized with β-catenin. Scale bars, 10 μm.

Each of the two mutations reported here affects crucial functions of αT-catenins. Mutant p.V94D protein interacts only weakly with β-catenin and plakoglobin, whereas the dimerization potential of mutant protein p.del765L is abnormally high, as shown by Y2H experiments and formation of aggresomes in transfected HEK293T cells. Though no studies on αT-catenin dimers vs. monomers have been reported, homodimeric forms of αE-catenin have been shown to bind to F-actin, whereas monomeric forms bind with greater strength to E-cadherin–β-catenin complexes.[17] We presume that in cardiomyocytes expressing the p.V94D or p.del765L mutant, higher levels of αT-catenin might be present in dimeric form outside the area composita. Moreover, as the mutant proteins can also heterodimerize with WT αT-catenin, they are expected to compete with the binding of WT αT-catenin to β-catenin and PKP2 within the area composita. We speculate that this might perturb F-actin organization at the ICD and simultaneously cause PKP2 to redistribute along the ICD. Our data indicate that αT-catenin cannot heterodimerize with αE-catenin, but the functionality of αE-catenin in the area composita might be indirectly affected by the change in F-actin dynamics owing to excessive αT-catenin dimerization. Nonetheless, the detailed expression patterns of various junctional components, including PKP2, in cardiomyocytes expressing αT-catenin mutations require further studies at higher resolution on more relevant material, i.e. endomyocardial biopsies or transgenic mouse models. Moreover, on the basis of the αT-catenin expression pattern and its specific function in the ICD, and in view of the *Ctnna3*-null mice phenotype, we expect that mutations in the *CTNNA3* gene will lead to a cardiac abnormality in humans. However, though our results provide evidence for the pathogenic role of the detected mutations, a limitation of the present study is the lack of the *in vivo* demonstration of their causative role. The proof of a causal relationship between *CTNNA3* mutations and ARVC awaits the generation and analysis of appropriate animal models, including knock-in mice for the various *Ctnna3* mutations.

In conclusion, our findings suggest a causal relationship between *CTNNA3* mutations and the ARVC pathology. The identification of a new gene involved in ARVC has major clinical implications. Since the frequency of CTNNA3 mutations in ARVC patients is not rare, systematic screening for this gene should be considered to improve the management of ARVC families, through early diagnosis and genetic-based cardiac screening and follow-up in relatives. Most mutations known to cause ARVC are in *JUP*, *DSP*, *PKP2*, *DSG2*, and *DSC2*, all of which encode proteins present in both desmosomes and areae compositae.[13] As αT-catenin is present only in areae compositae but not in desmosomes, ARVC could be considered a disease of the area composita rather than a classical desmosomal disease. Details of the role of αT-catenin in the ICD *in vivo* and of the behaviour of the mutant αT-catenin proteins identified in ARVC patients remain challenging topics of further study.

Supplementary material

Supplementary material is available at *European Heart Journal* online.

Acknowledgements

We thank Dr Steven Goossens, Dr Karl Vandepoele, Dr Vera Goossens, and Mrs Eef Parthoens for helpful discussions, Mrs Paola Marcon for her help in collecting ARVC families, Dr Marco Mongillo for providing neonatal rat cardiomyocytes, and Dr Amin Bredan for careful editing of the manuscript.

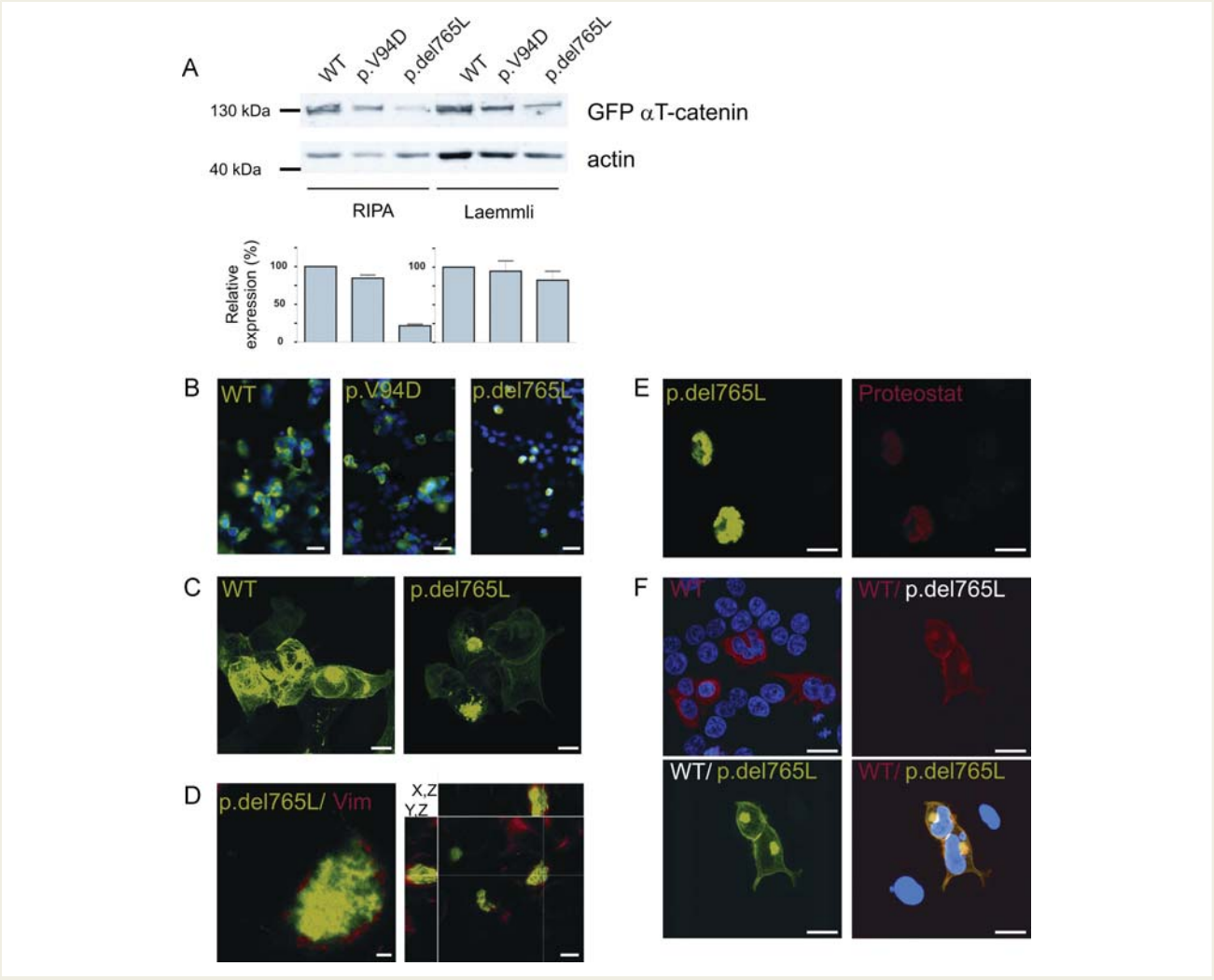

Figure 5 The p.del765L mutation promotes aggregation. (*A*) The recovery of overexpressed soluble WT and mutant αT-catenin proteins by two different lysis methods. HEK293T cells were transfected with plasmids expressing αT-catenin constructs (as indicated) and lysed 18 h later in either RIPA or Laemmli buffer. A representative western blot is shown. The experiment was repeated three times. The quantification of soluble GFP-αT-catenin protein expression relative to the actin band was performed using the LI-COR Odyssey software and is shown in the bottom panel (WT expression levels are taken as 100%). Standard errors of the average are shown for three independent experiments. In RIPA buffer only one-fifth of the p.del765L protein is soluble when compared with WT and p.V94D proteins. A paired two-tailed *t*-test showed that the differences are significant ($P < 0.001$). In Laemmli buffer, the p.del765L protein shows solubility comparable with this of WT and p.V94D protein. (*B* and *C*) Fluorescent images of HEK293T cells transfected with constructs expressing GFP-fused WT αT-catenin, p.V94D mutant, or p.del765L. The right panels show p.del765L aggregates (aggresomes) that are not present in cells expressing WT protein or p.V94D mutant. In (*B*) DNA was stained with DAPI (blue). (*D*) The p.del765L-induced aggresome formation in HEK293T cells is regularly accompanied by reorganization of the vimentin cytoskeleton. Note the cage-like appearance of vimentin fluorescence (red) in one confocal plane (left) and in three-dimensional reconstruction (right). (*E*) All p.del765L-induced aggresomes (green) stain positively with Proteostat (red), which is an aggresome detection reagent. (*F*) HEK293T cells transfected either with a single construct expressing Myc-tagged WT αT-catenin (upper left image) or with two constructs expressing Myc-tagged WT αT-catenin and GFP-fused p.del765L mutant (the three other images, of which lower right is a merged one). The contransfection shows that WT αT-catenin is colocalizing with mutant protein in the p.del765L-induced aggresomes. Scale bars: (*B*) 30 μm; (*C*) 10 μm; (*D*, left), 2 μm; (*D*, right), 10 μm; (*E*) 10 μm; (*F*) 20 μm.

Funding

This work was supported by the Research Foundation - Flanders (FWO) and the Concerted Research Actions - Ghent University (GOA) grants to F.v.R., and by TELETHON, Rome GGP09293, Fondazione CARIPARO, Padua, and AFM, Paris, grant 14776 to A.R.

Conflict of interest: none declared.

References

1. Marcus FI, Fontaine GH, Guiraudon G, Frank R, Laurenceau JL, Malergue C, Grosgogeat Y. Right ventricular dysplasia: a report of 24 adult cases. *Circulation* 1982;**65**:384–398.

2. Thiene G, Nava A, Corrado D, Rossi L, Pennelli N. Right ventricular cardiomyopathy and sudden death in young people. *N Engl J Med* 1988;**318**:129–133.
3. Nava A, Thiene G, Canciani B, Scognamiglio R, Daliento L, Buja G, Martini B, Stritoni P, Fasoli G. Familial occurrence of right ventricular dysplasia: a study involving nine families. *J Am Coll Cardiol* 1988;**12**:1222–1228.
4. Protonotarios N, Tsatsopoulou A. Naxos disease: cardiocutaneous syndrome due to cell adhesion defect. *Orphanet J Rare Dis* 2006;**1**:4.
5. Alcalai R, Metzger S, Rosenheck S, Meiner V, Chajek-Shaul T. A recessive mutation in desmoplakin causes arrhythmogenic right ventricular dysplasia, skin disorder, and woolly hair. *J Am Coll Cardiol* 2003;**42**:319–327.
6. McKoy G, Protonotarios N, Crosby A, Tsatsopoulou A, Anastasakis A, Coonar A, Norman M, Baboonian C, Jeffery S, McKenna WJ. Identification of a deletion in plakoglobin in arrhythmogenic right ventricular cardiomyopathy with palmoplantar keratoderma and woolly hair (Naxos disease). *Lancet* 2000;**355**:2119–2124.
7. Rampazzo A, Nava A, Malacrida S, Beffagna G, Bauce B, Rossi V, Zimbello R, Simionati B, Basso C, Thiene G, Towbin JA, Danieli GA. Mutation in human desmoplakin domain binding to plakoglobin causes a dominant form of arrhythmogenic right ventricular cardiomyopathy. *Am J Hum Genet* 2002;**71**:1200–1206.
8. Gerull B, Heuser A, Wichter T, Paul M, Basson CT, McDermott DA, Lerman BB, Markowitz SM, Ellinor PT, MacRae CA, Peters S, Grossmann KS, Michely B, Sasse-Klaassen S, Birchmeier W, Dietz R, Breithardt G, Schulze-Bahr E, Thierfelder L. Mutations in the desmosomal protein plakophilin-2 are common in arrhythmogenic right ventricular cardiomyopathy. *Nat Genet* 2004;**36**:1162–1164.
9. Pilichou K, Nava A, Basso C, Beffagna G, Bauce B, Lorenzon A, Frigo G, Vettori A, Valente M, Towbin J, Thiene G, Danieli GA, Rampazzo A. Mutations in desmoglein-2 gene are associated with arrhythmogenic right ventricular cardiomyopathy. *Circulation* 2006;**113**:1171–1179.
10. Syrris P, Ward D, Evans A, Asimaki A, Gandjbakhch E, SenChowdhry S, McKenna WJ. Arrhythmogenic right ventricular dysplasia/cardiomyopathy associated with mutations in the desmosomal gene desmocollin- 2. *Am J Hum Genet* 2006;**79**:978–984.
11. Asimaki A, Syrris P, Wichter T, Matthias P, Saffitz JE, McKenna WJ. A novel dominant mutation in plakoglobin causes arrhythmogenic right ventricular cardiomyopathy. *Am J Hum Genet* 2007;**81**:964–973.
12. Basso C, Bauce B, Corrado D, Thiene G. Pathophysiology of arrhythmogenic cardiomyopathy. *Nat Rev Cardiol* 2011;**9**:223–233.
13. Borrmann CM, Grund C, Kuhn C, Hofmann I, Pieperhoff S, Franke WW. The area composita of adhering junctions connecting heart muscle cells of vertebrates. II. Colocalizations of desmosomal and fascia adhaerens molecules in the intercalated disk. *Eur J Cell Biol* 2006;**85**:469–485.
14. van Roy F, Berx G. The cell-cell adhesion molecule E-cadherin. *Cell Mol Life Sci* 2008;**65**:3756–3788.
15. Maiden SL, Hardin J. The secret life of alpha-catenin: moonlighting in morphogenesis. *J Cell Biol* 2011;**195**:543–552.
16. Yamada S, Pokutta S, Drees F, Weis WI, Nelson WJ. Deconstructing the cadherin-catenin-actin complex. *Cell* 2005;**123**:889–901.
17. Drees F, Pokutta S, Yamada S, Nelson WJ, Weis WI. alpha-catenin is a molecular switch that binds E-cadherin- beta-catenin and regulates actin-filament assembly. *Cell* 2005;**123**:903–915.
18. Janssens B, Goossens S, Staes K, Gilbert B, van Hengel J, Colpaert C, Bruyneel E, Mareel M, van Roy F. αT-Catenin: a novel tissue-specific β-catenin-binding protein mediating strong cell-cell adhesion. *J Cell Sci* 2001;**114**:3177–3188.
19. Goossens S, Janssens B, Bonné S, De Rycke R, Braet F, van Hengel J, van Roy F. A unique and specific interaction between alpha-T-catenin and plakophilin-2 recruits desmosomal proteins to the adherens junctions of the heart. *J Cell Sci* 2007;**120**:2126–2136.
20. Marcus FI, McKenna WJ, Sherrill D, Basso C, Bauce B, Bluemke DA, Calkins H, Corrado D, Cox MG, Daubert JP, Fontaine G, Gear K, Hauer R, Nava A, Picard MH, Protonotarios N, Saffitz JE, Sanborn DM, Steinberg JS, Tandri H, Thiene G, Towbin JA, Tsatsopoulou A, Wichter T, Zareba W. Diagnosis of arrhythmogenic right ventricular cardiomyopathy/dysplasia: proposed modification of the Task Force Criteria. *Eur Heart J* 2010;**31**:806–814.
21. Gietz RD, Schiestl RH, Willems AR, Woods RA. Studies on the transformation of intact yeast cells by the LiAc/SS-DNA/PEG procedure. *Yeast* 1995;**11**:355–360.
22. Zaccolo M, Pozzan T. Discrete microdomains with high concentration of cAMP in stimulated rat neonatal cardiac myocytes. *Science* 2002;**295**:1711–1715.
23. Knop M, Siegers K, Pereira G, Zachariae W, Winsor B, Nasmyth K, Schiebel E. Epitope tagging of yeast genes using a PCR-based strategy: more tags and improved practical routines. *Yeast* 1999;**15**:963–972.
24. Bauce B, Basso C, Rampazzo A, Beffagna G, Daliento L, Frigo G, Malacrida S, Settimo L, Danieli G, Thiene G, Nava A. Clinical profile of four families with arrhythmogenic right ventricular cardiomyopathy caused by dominant desmoplakin mutations. *Eur Heart J* 2005;**26**:1666–1675.
25. Kobielak A, Fuchs E. Alpha-catenin: at the junction of intercellular adhesion and actin dynamics. *Nat Rev Mol Cell Biol* 2004;**5**:614–625.
26. Johnston JA, Ward CL, Kopito RR. Aggresomes: a cellular response to misfolded proteins. *J Cell Biol* 1998;**143**:1883–1898.
27. Shen D, Coleman J, Chan E, Nicholson TP, Dai L, Sheppard PW, Patton WF. Novel cell- and tissue-based assays for detecting misfolded and aggregated protein accumulation within aggresomes and inclusion bodies. *Cell Biochem Biophys* 2011;**60**:173–185.
28. Beaudoin S, Goggin K, Bissonnette C, Grenier C, Roucou X. Aggresomes do not represent a general cellular response to protein misfolding in mammalian cells. *BMC Cell Biol* 2008;**9**:59.
29. Janssens B, Mohapatra B, Vatta M, Goossens S, Vanpoucke G, Kools P, Montoye T, van Hengel J, Bowles NE, van Roy F, Towbin JA. Assessment of the *CTNNA3* gene encoding human alphaT-catenin regarding its involvement in dilated cardiomyopathy. *Hum Genet* 2003;**112**:227–236.
30. Christensen AH, Benn M, Tybjaerg-Hansen A, Haunso S, Svendsen JH. Screening of three novel candidate genes in arrhythmogenic right ventricular cardiomyopathy. *Genet Test Mol Biomarkers* 2011;**15**:267–271.
31. Li J, Goossens S, van Hengel J, Gao E, Cheng L, Tyberghein K, Shang X, De Rycke R, van Roy F, Radice G. Loss of alpha-T-catenin alters the hybrid adhering junctions in the heart and leads to dilated cardiomyopathy and ventricular arrhythmia following acute ischemia. *J Cell Sci* 2012;**125**:1058–1067.